Journal of Computational Methods in Molecular Design, 2012, 2 (3):99-106

Scholars Research Library
(http://scholarsresearchlibrary.com/archive.html)

ISSN : 2231- 3176
CODEN (USA): JCMMDA

Quantitative structure-activity relationship study of benzene sulfonamides as inhibitor of carbonic anhydrase based on quantum chemical descriptor

Praveen Srivastava, Shailly Srivastava, Anil Kumar Soni and Rajesh Kumar Singh

Department of Chemistry, Maharani Lal Kunwari Post Graduate College, Balrampur (U.P.), INDIA

ABSTRACT

Quantitative structure-activity relationship of twenty nine benzene sulfonamides as inhibitor of carbonic anhydrase based on quantum chemical descriptor, heat of formation, molecular weight, total energy, energy of highest occupied molecular orbital, energy of lowest unoccupied molecular orbital, electronegativity and absolute hardness, has been studied. The purpose of the study is to test the suitability of the above quantum chemical parameters as possible biological activity descriptor in the development of QSAR. We have considered 83 QSAR models using, multiple linear regression, MLR, analysis with the help of various combinations of the descriptors. In order to explore the reliability of the proposed model we have used regression coefficient, r^2, and cross-validation coefficient, rCV^2. The study shows that heat of formation, molecular weight, total energy and energy of highest occupied molecular orbitals of the benzene sulfonamides can be used as descriptors of biological activity.

Keywords: Benzene sulfonamides, QSAR, quantum chemical descriptor and carbonic anhydrase

---

INTRODUCTION

Carbonic anhydrase (CA) catalyzes the inter-conversion of carbon dioxide to biocarbonate. There are three classes α, β, and γ of CA, divided into three genetically unrelated families, namely, animal, plant, and bacterial CAs, respectively [1,2]. There is no amino acid homology between classes [3], although there is some overlap of the occurrence of the genes. At the present, it is believed that only the α-genes are present in vertebrate organisms. The tissue distribution of α-CA seems to be ubiquitous with cytoplasmic, transmembrane, mitochondrial, secreted form. CA II is the most extensively studied isozyme of CA and has a wide tissue distribution and can be found in some cells of virtually every tissue type with large amounts located in the red blood cells where it is involved in respiration. CA II with its wide tissue distribution has varied physiological roles throughout the body. In addition to catalyzing the reversible hydration of CO_2 and HCO_3^- from respiration, CA II also acidifies urine by eliminating H^+ in the renal tubules and collecting ducts of the kidney, provides H^+ necessary for the bone resorption function of osteoclasts, produces HCO_3^- for use in pyrimidine biosynthesis, supplies H^+ and maintains pH balance in the choroid plexus for cerebro spinal fluid (CSF) formation, involved in saliva production by producing HCO_3^- for acinar and ductal cells, provides H^+ to gastral parietal cells for stomach acidification, and provides HCO_3^- to liver epithelial duct cells for bile production and to epithelial duct cells of the pancreas for pancreatic juice formation. A specific clinical phenotype has been noted for CA II deficiency – osteopetrosis and renal tubular acidosis, which in some cases is accompanied by mental retardation [4]. CA catalyses the interconversion of CO_2 to HCO_3^- in a two-stage ping-pong reaction. Human CA II (hCA II) catalyzes the reversible hydration of CO_2 in two distinct half reactions [5, 6]. The first step of the reaction involves the tapping of the CO_2 substrate within a putative hydrophobic pocket [7]. The CO_2 displaces a water molecule, 'the deep water', in the active site by associating with the amide nitrogen of Thr199 in a hydrogen-bonding interaction prior to a nucleophilic attack on the substrate carbon to form biocarbonate (Figure 1). The bicarbonate is then displaced from the zinc ion by an active-site water molecule, concluding the first-half (Equation (a)).

$$CO_2 + EZnOH^- \rightleftharpoons EZnHCO_3^- \overset{H_2O}{\rightleftharpoons} EZnH_2O + HCO_3^- \quad (a)$$

$$EZnH_2O + B \rightleftharpoons EZnOH^- + BH^- \quad (b)$$

The second-half reaction involves the transfer of a proton from the zinc-bound water molecule to residue His64 through a chain of hydrogen-bonded water molecules [6,8]. This intramolecular proton transfer is followed by an intermolecular proton transfer from His64 to bulk solvent (B) of the system. This second step regenerates the zinc-bound hydroxyl group, allowing for another round of catalysis to proceed (Equation (b), Figure 1).

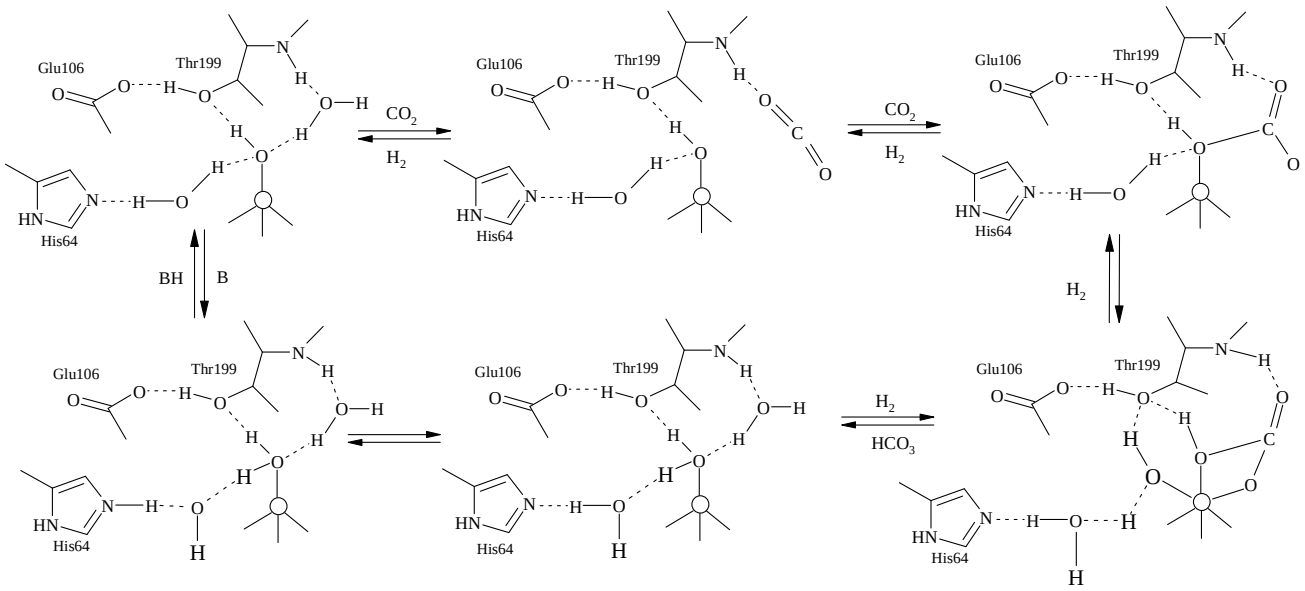

Figure 1. Schematic representation of the catalytic mechanism of carbonic anhydrase.

Inorganic and organic anions have been useful in studying the properties of the metal center in carbonic anhydrase. Most monovalent anions inhibit CA with varying affinities. These inhibitors bind to the metal ion and disrupt the coordination of the zinc-OH^- group that disrupts the catalytic activity of the enzyme [9]. Since the discovery, 61 years ago, that sulphonamides inhibit CA, powerful inhibitors of CA have been restricted to the structure RSO_2NH_2 where R is an aromatic or heteroaromatic residue [10]. Parenteral sulfonamides (i.e.,acetazolamide, methazolamide, dichlorphenamide, and ethoxazolamide) have been used for 45 years to reduce intraocular pressure in glaucoma. Their pharmacological effect is believed to be due to the inhibition of CA II in the ciliary epithelium. Unfortunately, systemic therapy with parenteral sulfonamides and their derivatives leads to significant side effects, many of which are probably due to inhibition of CA isoforms in other tissues. These undesirable side effects call for the synthesis of new derivatives of sulfonamides that are more selective against CA II to be used in glaucoma treatment [11]. But this research work is confined to study of following twenty nine derivatives of benzene sulfonamide listed in Table 1. In this work, six quantum chemical descriptors: heat of formation (ΔH_f° in $kcalmol^{-1}$) [12], molecular weight (MW) [13], total energy (TE in Hartree) [14], HOMO energy ($\in$HOMO in eV) [15], LUMO energy ($\in$LUMO in eV) [15], electronegativity (χ) [16] and absolute hardness (η) [17] have been used for QSAR [18, 19] study of twenty nine derivatives of benzene sulfonamide [20] (Figure-1). Because of the huge, and well-defined physical information encoded in many theoretical descriptors [21], their use in the design of a training set in a QSAR study presents two main advantages: (a) the compounds and their various fragments and substituents can be directly characterized on the basis of their molecular structure only; and (b) the proposed mechanism of action can be directly accounted for the chemical reactivity of the compounds under study. Consequently, the derived QSAR models will include information regarding the nature of the intermolecular forces involved in determining the biological or other activity of the compounds in question.

MATERIALS AND METHODS

The study materials of this paper are twenty nine derivatives of benzene sulfonamide and are presented in Table-1 [20].

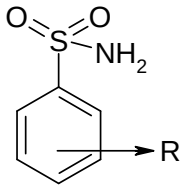

Table 1. Derivatives of benzene sulfonamides

No.	R	log K	No.	R	log K
1	H	6.69	16	4-$CONHC_4H_9$	8.49
2	4-CH_3	7.09	17	4-$CONHC_5H_{11}$	8.75
3	4-C_2H_5	7.53	18	4-$CONHC_6H_{13}$	8.88
4	4-C_3H_7	7.77	19	4-$CONHC_7H_{15}$	8.93
5	4-C_4H_9	8.30	20	3-CO_2CH_3	5.87
6	4-C_5H_{11}	8.86	21	3-$CO_2C_2H_5$	6.21
7	4-CO_2CH_3	7.99	22	3-$CO_2C_3H_7$	6.44
8	4-$CO_2C_2H_5$	8.50	23	3-$CO_2C_4H_9$	6.95
9	4-$CO_2C_3H_7$	8.77	24	3-$CO_2C_5H_{11}$	6.86
10	4-$CO_2C_4H_9$	9.11	25	2-CO_2CH_3	4.41
11	4-$CO_2C_5H_{11}$	9.39	26	2-$CO_2C_2H_5$	4.80
12	4-$CO_2C_6H_{13}$	9.39	27	2-$CO_2C_3H_7$	5.28
13	4-$CONHCH_3$	7.08	28	2-$CO_2C_4H_9$	5.76
14	4-$CONHC_2H_5$	7.53	29	2-$CO_2C_5H_{11}$	6.18
15	4-$CONHC_3H_7$	8.08			

Where log K is binding constants of benzene sulfonamides to CA

For QSAR prediction, the structures of all the above compounds have been drawn and their geometries have been optimized with the help of CAChe software [22] using PM3 hamiltonian [23]. MOPAC calculations have been performed with MOPAC 2002 software [24] associated with CAChe.

The values of above descriptors have been obtained from this software by solving the equations given below and the results are included in Table 2.

The heat of formation [12] is defined as

$$\Delta H_f^o = E_{elect} + E_{nuc} - E_{isol} + E_{atom} \qquad \text{Eq.I}$$

where E_{elect} is the electronic energy, E_{nuc} is the nuclear-nuclear repulsion energy, E_{isol} is the energy required to strip all the valence electrons of all the atoms in the system and E_{atom} is the total heat of atomization of all the atoms in the system.

The molecular weight (MW) [13] is a more general, but important, property of a molecular system and has also been tested as descriptor.

Total energy (TE) [14] of a molecular system is the sum of the total electronic energy, E_{ee} and the energy of internuclear repulsion, E_{nr}. The total electronic energy of the system is given by

$$E = \frac{P(H+F)}{2} \qquad \text{Eq.II}$$

where P is the density matrix and H is the one-electron matrix.

Parr et al. defined electronegativity [16] as the negative of chemical potential:

$$\chi = -\mu = -\left(\frac{\delta E}{\delta N}\right)_{V(r)} \qquad \text{Eq.III}$$

The absolute hardness (η) [6] is defined as

$$\eta = \frac{1}{2}\left(\frac{\delta \mathrm{E}}{\delta \mathrm{N}}\right)_{V(r)}$$

$$\eta = \frac{1}{2}\left(\frac{\delta^2 \mathrm{E_T}}{\delta \mathrm{N}^2}\right)_{V(r)} \qquad \text{Eq.IV}$$

where E_T is the total energy, N the number of electrons of the chemical species and v(r) the external potential. The operational definition of absolute hardness and electronegativity is defined as

$$\eta = \frac{(IP - EA)}{2} \qquad \text{Eq.V}$$

$$\chi = -\mu = \frac{(IP + EA)}{2} \qquad \text{Eq.VI}$$

where IP and EA are the ionization potential and electron affinity respectively, of the chemical species. According to the Koopman's theorem, the IP is simply the eigen value of the HOMO with change of sign and the EA is the eigen value of the LUMO with change of sign hence the Eq.V and VI can be written as

$$\eta = \frac{(\varepsilon LUMO - \varepsilon HOMO)}{2} \qquad \text{Eq.VII}$$

$$\chi = \frac{(\varepsilon LUMO + \varepsilon HOMO)}{2} \qquad \text{Eq.VIII}$$

Table 2. Calculation of various quantum chemical descriptors of the compounds with OBA

No.	ΔH_f (kcal/mole)	MW	TE (Hartree)	∈HOMO (eV)	∈LUMO (eV)	η	χ	OBA (logK)
1	106.162	157.187	-79.969	-9.552	-1.883	3.834	-5.717	6.690
2	96.482	171.214	-87.159	-9.493	-1.843	3.825	-5.668	7.090
3	92.863	185.240	-94.316	-9.488	-1.837	3.826	-5.662	7.530
4	86.654	199.267	-101.480	-9.504	-1.849	3.827	-5.676	7.770
5	81.232	213.294	-108.640	-9.512	-1.848	3.832	-5.680	8.300
6	75.801	227.321	-115.799	-9.510	-1.849	3.830	-5.680	8.860
7	130.385	215.223	-116.676	-9.596	-2.289	3.654	-5.942	7.980
8	126.307	229.250	-123.836	-9.491	-2.330	3.581	-5.910	8.500
9	120.832	243.277	-131.001	-9.647	-2.261	3.693	-5.954	8.770
10	115.431	257.304	-138.162	-9.648	-2.260	3.694	-5.954	9.110
11	110.005	271.331	-145.322	-9.648	-2.261	3.694	-5.955	9.390
12	104.579	285.357	-152.482	-9.650	-2.260	3.695	-5.955	9.390
13	67.316	214.239	-114.025	-9.663	-2.097	3.783	-5.880	7.080
14	61.140	228.265	-121.177	-9.657	-2.088	3.785	-5.872	7.530
15	55.895	242.292	-128.337	-9.657	-2.089	3.784	-5.873	9.080
16	50.468	256.319	-135.497	-9.655	-2.089	3.783	-5.872	8.490
17	45.049	270.346	-142.657	-9.654	-2.089	3.782	-5.872	8.750
18	39.618	284.373	-149.817	-9.653	-2.089	3.782	-5.871	8.880
19	34.189	298.399	-156.977	-9.656	-2.089	3.783	-5.873	8.930
20	130.284	215.223	-116.674	-9.656	-2.189	3.733	-5.922	5.870
21	125.830	229.250	-123.837	-9.691	-2.201	3.745	-5.946	6.210
22	120.767	243.277	-130.993	-9.555	-2.186	3.684	-5.870	6.440
23	114.893	257.304	-138.158	-9.688	-2.198	3.745	-5.943	6.950
24	109.471	271.331	-145.318	-9.689	-2.198	3.745	-5.944	6.860
25	134.094	215.223	-116.669	-9.775	-2.200	3.787	-5.988	4.410
26	130.199	229.250	-123.834	-9.792	-2.189	3.802	-5.990	4.800
27	124.769	243.277	-130.994	-9.788	-2.186	3.801	-5.987	5.280
28	119.353	257.304	-138.155	-9.788	-2.187	3.801	-5.987	5.760
29	113.933	271.331	-145.315	-9.789	-2.187	3.801	-5.988	6.180

$\Delta H_f°$ is heat of formation, MW is molecular weight, TE is total energy, ∈HOMO is energy of highest occupied molecular orbital, ∈LUMO is energy of lowest unoccupied molecular orbital, η is absolute hardness, χ is electronegativity and log K is binding constants of benzene sulfonamides to CA

RESULTS AND DISCUSSION

Based on above quantum chemical descriptors, the QSAR model of twenty nine derivatives of benzene sulfonamide has been studied. The purpose of the study is to test the suitability of the above quantum chemical parameters as possible biological activity descriptor in the development of QSAR. In developing QSAR models, quantum chemical descriptors used as independent variables and the observed biological activity in term of log K values as dependent variable. We have considered 83 QSAR models using MLR analysis[25-27] with the help of various combinations of the descriptors shown in Table-3. The quantities of descriptors have been taken from Table-2.

Table 3. Combination of descriptors for MLR analysis

Predicted Activity	First descriptor	Second descriptor	Third descriptor	Fourth descriptor
SPA1	Heat of Formation	Molecular Weight		
SPA2	Heat of Formation	Total Energy		
SPA3	Heat of Formation	HOMO Energy		
SPA4	Heat of Formation	LUMO Energy		
SPA5	Heat of Formation	Electronegativity		
SPA6	Heat of Formation	Absolute Hardness		
SPA7	Molecular Weight	Total Energy		
SPA8	Molecular Weight	HOMO Energy		
SPA9	Molecular Weight	LUMO Energy		
SPA10	Molecular Weight	Electronegativity		
SPA11	Molecular Weight	Absolute Hardness		
SPA12	Total Energy	HOMO Energy		
SPA13	Total Energy	LUMO Energy		
SPA14	Total Energy	Electronegativity		
SPA15	Total Energy	Absolute Hardness		
SPA16	HOMO Energy	LUMO Energy		
SPA17	HOMO Energy	Electronegativity		
SPA18	HOMO Energy	Absolute Hardness		
SPA19	LUMO Energy	Electronegativity		
SPA20	LUMO Energy	Absolute Hardness		
SPA21	Electronegativity	Absolute Hardness		
SPA22	Heat of Formation	Molecular Weight	Total Energy	
SPA23	Heat of Formation	Molecular Weight	HOMO Energy	
SPA24	Heat of Formation	Molecular Weight	LUMO Energy	
SPA25	Heat of Formation	Molecular Weight	Electronegativity	
SPA26	Heat of Formation	Molecular Weight	Absolute Hardness	
SPA27	Molecular Weight	Total Energy	HOMO Energy	
SPA28	Molecular Weight	Total Energy	LUMO Energy	
SPA29	Molecular Weight	Total Energy	Electronegativity	
SPA30	Molecular Weight	Total Energy	Absolute Hardness	
SPA31	Total Energy	HOMO Energy	LUMO Energy	
SPA32	Total Energy	HOMO Energy	Electronegativity	
SPA33	Total Energy	HOMO Energy	Absolute Hardness	
SPA34	HOMO Energy	LUMO Energy	Electronegativity	
SPA35	HOMO Energy	LUMO Energy	Absolute Hardness	
SPA36	LUMO Energy	Electronegativity	Absolute Hardness	
SPA37	Molecular Weight	HOMO Energy	LUMO Energy	
SPA38	Molecular Weight	HOMO Energy	Electronegativity	
SPA39	Molecular Weight	HOMO Energy	Absolute Hardness	
SPA40	Molecular Weight	LUMO Energy	Electronegativity	
SPA41	Molecular Weight	LUMO Energy	Absolute Hardness	
SPA42	Molecular Weight	Electronegativity	Absolute Hardness	
SPA43	Total Energy	LUMO Energy	Electronegativity	
SPA44	Total Energy	LUMO Energy	Absolute Hardness	
SPA45	Total Energy	Electronegativity	Absolute Hardness	
SPA46	Heat of Formation	Total Energy	HOMO Energy	
SPA47	Heat of Formation	Total Energy	LUMO Energy	
SPA48	Heat of Formation	Total Energy	Electronegativity	
SPA49	Heat of Formation	Total Energy	Absolute Hardness	
PSA50	Heat of Formation	HOMO Energy	LUMO Energy	
SPA51	Heat of Formation	HOMO Energy	Electronegativity	
SPA52	Heat of Formation	Total Energy	HOMO Energy	Absolute Hardness
SPA53	Heat of Formation	LUMO Energy	Electronegativity	
SPA54	Heat of Formation	LUMO Energy	Absolute Hardness	
SPA55	Heat of Formation	Electronegativity	Absolute Hardness	
SPA56	HOMO Energy	Electronegativity	Absolute Hardness	
SPA57	Heat of Formation	Molecular Weight	Total Energy	HOMO Energy
SPA58	Heat of Formation	Molecular Weight	Total Energy	LUMO Energy
SPA59	Heat of Formation	Molecular Weight	Total Energy	Electronegativity
SPA60	Heat of Formation	Molecular Weight	Total Energy	Absolute Hardness
SPA61	Heat of Formation	Molecular Weight	HOMO Energy	LUMO Energy

SPA62	Heat of Formation	Molecular Weight	HOMO Energy	Electronegativity
SPA63	Heat of Formation	Molecular Weight	HOMO Energy	Absolute Hardness
SPA64	Heat of Formation	Molecular Weight	LUMO Energy	Electronegativity
SPA65	Heat of Formation	Molecular Weight	LUMO Energy	Absolute Hardness
SPA66	Heat of Formation	Molecular Weight	Electronegativity	Absolute Hardness
SPA67	Molecular Weight	Total Energy	HOMO Energy	LUMO Energy
SPA68	Molecular Weight	Total Energy	HOMO Energy	Electronegativity
SPA69	Molecular Weight	Total Energy	HOMO Energy	Absolute Hardness
SPA70	Molecular Weight	Total Energy	LUMO Energy	Electronegativity
SPA71	Molecular Weight	Total Energy	LUMO Energy	Absolute Hardness
SPA72	Molecular Weight	Total Energy	Electronegativity	Absolute Hardness
SPA73	Molecular Weight	Total Energy	LUMO Energy	Electronegativity
SPA74	Molecular Weight	Total Energy	LUMO Energy	Absolute Hardness
SPA75	Total Energy	HOMO Energy	Electronegativity	Absolute Hardness
SPA76	HOMO Energy	LUMO Energy	Electronegativity	Absolute Hardness
SPA77	Heat of Formation	Total Energy	HOMO Energy	LUMO Energy
SPA78	Heat of Formation	Total Energy	HOMO Energy	Electronegativity
SPA79	Heat of Formation	Total Energy	HOMO Energy	Absolute Hardness
SPA80	Heat of Formation	Total Energy	LUMO Energy	Electronegativity
SPA81	Heat of Formation	Total Energy	LUMO Energy	Absolute Hardness
SPA82	Heat of Formation	HOMO Energy	LUMO Energy	Electronegativity
SPA83	Heat of Formation	HOMO Energy	LUMO Energy	Absolute Hardness

In order to explore the reliability of the proposed model we have used regression coefficient (r^2) and cross-validation coefficient (rCV^2). Out of above 83 QSAR models only 51 models have predictive powers as these have higher values (»0.5) of both rCV^2 and r^2 coefficients, while the rest have either the value of rCV^2 («0.2) or r^2 («0.5) or both much lower than their optimum values. Out of 51 models the top five models are as below:

I. Top first reliable QSAR model: The top first QSAR model is obtained when multi linear regression analysis is done by taking heat of formation as first descriptor, molecular weight as second descriptor, total energy as third descriptor and LUMO energy as fourth descriptor. The regression equation is given below:

$$SPA58=-0.0193872 \times \Delta H_f^{\circ} +0.871599 \times MW +1.66239 \times TE -27.8945 \times \in LUMO -47.0456$$

rCV^2=0.682865

r^2=0.848966 Eq.58

II. Top second reliable QSAR model: The top second QSAR model is obtained when multi linear regression analysis is done by taking heat of formation as first descriptor, molecular weight as second descriptor, total energy as third descriptor and electronegativity as fourth descriptor. The regression equation is given below:

$$SPA59=-0.0170746 \times \Delta H_f^{\circ} +0.278119 \times MW +0.498118 \times TE -20.3694 \times \chi +82.5278$$

rCV^2=0.56173

r^2=0.840678 Eq.59

III. Top third reliable QSAR model: The top third QSAR model is obtained when multi linear regression analysis is done by taking molecular weight as first descriptor, total energy as second descriptor, HOMO energy as third descriptor and LUMO energy as fourth descriptor. The regression equation is given below:

$$SPA67=0.677959 \times MW +1.25548 \times TE +5.51786 \times \in HOMO -18.9981 \times \in LUMO +17.7615$$

rCV^2=0.584151

r^2=0.816355 Eq.67

IV. Top fourth reliable QSAR model: The top fourth QSAR model is obtained when multi linear regression analysis is done by taking molecular weight as first descriptor, total energy as second descriptor, HOMO energy as third descriptor and electronegativity as fourth descriptor. The regression equation is given below:

$$SPA68=0.677959 \times MW +1.25548 \times TE -13.4802 \times \in HOMO -37.9962 \times \chi +17.7615$$

rCV^2=0.584151

r^2=0.816355 Eq.68

V. Top fifth reliable QSAR model: The top fifth QSAR model is obtained when multi linear regression analysis is done by taking molecular weight as first descriptor, total energy as second descriptor, HOMO energy as third descriptor and absolute hardness as fourth descriptor. The regression equation is given below:

SPA69=0.677959 × MW +1.25548 × TE +24.516 × ∈HOMO -37.9962 × η +17.7615
rCV^2=0.584151

r^2=0.816355 Eq.69

The grammatical representation of relationships between the predicted binding constant and observed binding constant are shown in Figure 2.

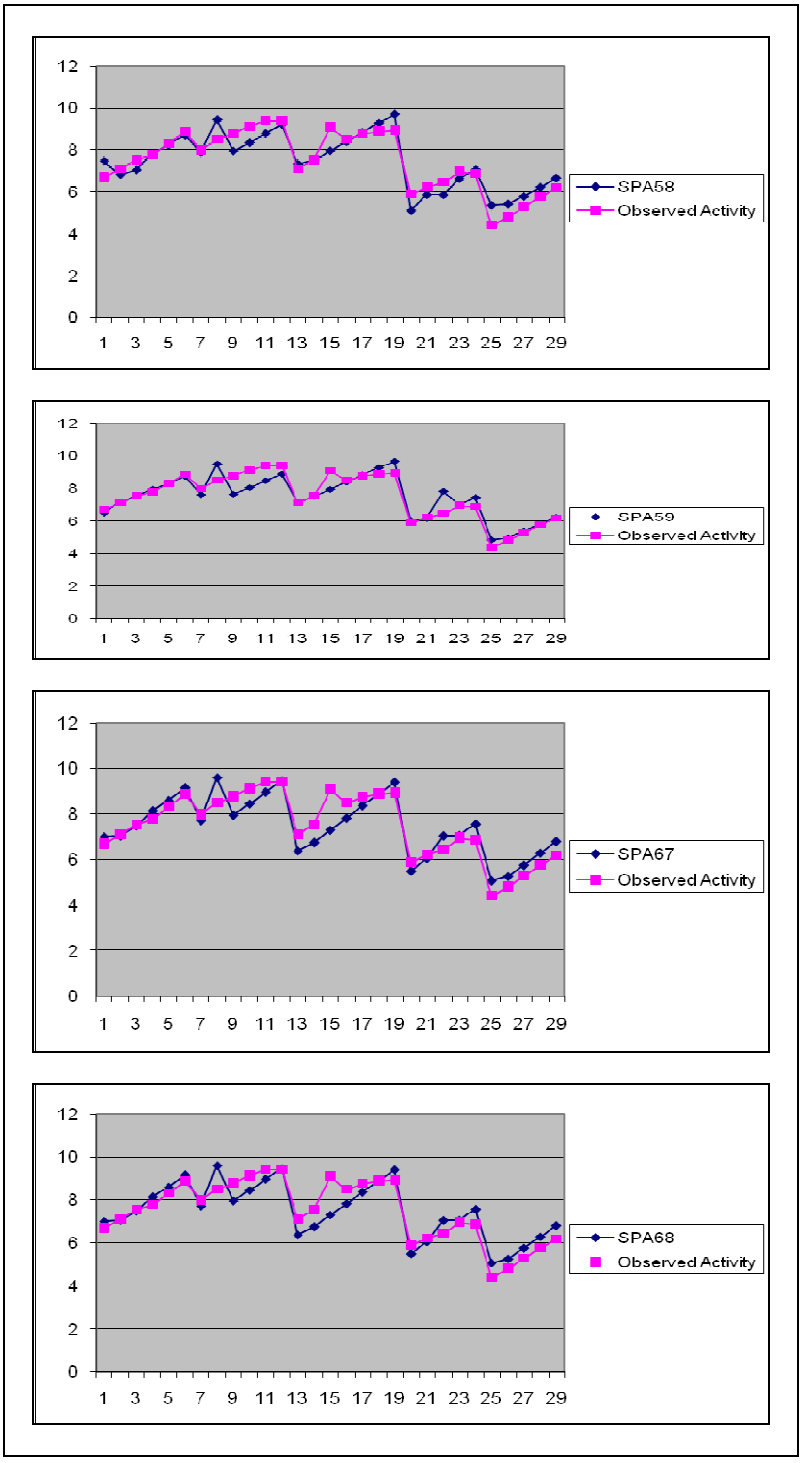

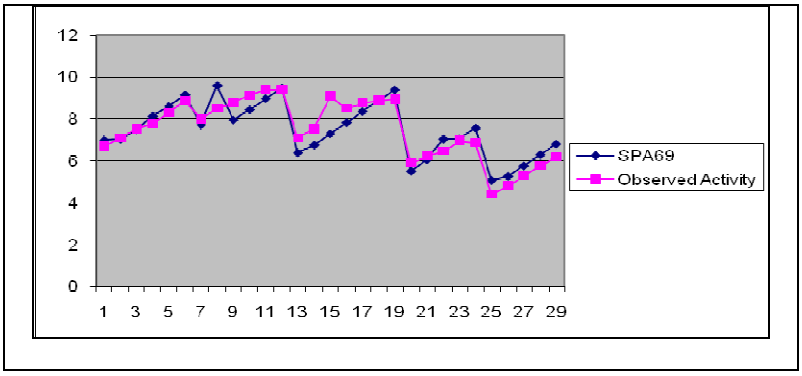

Figure 2. Graph between predicted and observed activity (logK)

CONCLUSION

The study shows that quantum chemical descriptors especially heat of formation, molecular weight, total energy and energy of highest occupied molecular orbitals of the benzene sulfonamides can be used as descriptors of biological activity. On the basis of the derived model, SPA58=-0.0193872 × ΔH_f° +0.871599 × MW +1.66239 × TE -27.8945 × ∈LUMO -47.0456, one can build up a theoretical basis to access the biological activity of the compounds of the same series.

REFERENCES

[1]. S. Parkkila in W. R. Chegwidden, N. D. Carter, Edwards, Y.H. (eds.), *Carbonic Anhydrase New Horizons: An Overview of the Distribution and Function of Carbonic Anhydrase in Mammals*, Birkhauser Verlag Basel, Switzerland, **2000,** pp 80-93.
[2]. B. Ulmasov, A. Waheed, G. N. Shah, J. H. Grubb, W. S. Sly, C. K. Tu, D. N. Silverman, *Proc. Natl. Acad. Sci. USA*, **2000,** 97, 14212.
[3]. D. Hewett-Emmett, R. E. Tashian, *Mol. Phylogenet. Evol.*, **2000,** 97, 14212.
[4]. W. S. Sly, P. Y. Hu, *Annu. Rev. Biochem.*, **1995,** 64, 375.
[5]. S. Lindskog, *Pharmacol. Ther.*, **1997,** 74, 1.
[6]. D. W. Christianson, C. A. Fierke, *Acc. Chem. Res.*, **1996,** 29, 331.
[7]. S. Lindskog, D. N. Silverman, in W. R. Chegwidden, N. D. Carter, Y. H. Edwards (eds.), *Carbonic Anhydrase New Horizons: An Overview of the Distribution and Function of Carbonic Anhydrase in Mammals*, Birkhauser Verlag Basel, Switzerland, **2000,** pp 175-95.
[8]. A. E. Eriksson, T. A. Jones, A. Liljas, *Proteins: Struct. Funct. Genet.*, **1988,** 4, 274.
[9]. I. Bertini, C. Luchinat, *Acc. Chem. Res.*, **1983,** 16, 272.
[10]. T. H. Maren, *Drug Des. Res.*, **1987,** 10, 255.
[11]. T. H. Maren, A. Barilan, K. C. Caster, A. R. Katritsky, *J. Pharmacol. Exp. Ther*., **1987,** 241, 56.
[12]. M. P. Badenes, M. E. Tucceri, C. J. Cobos, *Zeitschrift für Physikalische Chemie* **2000**, 214, 1193.
[13]. F. A. Pasha, H. K. Srivastava, P. P. Singh, *Bioorg. & Med. Chem.* **2005**, 13, 6823.
[14]. V. K. Sahu, A. K. Soni, P. P. Singh, *Asian J. Chem.* **2010**, 22, 3025.
[15]. G. Klopman, *J. Am. Chem. Soc.* **1968**, 90, 223.
[16]. R. G. Pearson, *Proc. Natl. Acad. Sci. USA.*, **1986**, 83, 8440.
[17]. R. G. Parr, R. G. Pearson, *J. Am. Chem. Soc.*, **1983**, 105, 7512.
[18]. C. Hansch, T. Fujita, *J. Am. Chem. Soc.* **1964**, *86*, 1616.
[19]. C. Hansch, A. Leo, Exploring QSAR. Washington, DC: *American Chemical Society*, **1995**.
[20]. C. T. Supuran, *Nat. Rev. Drug Discov.*, **2008,** *7*, 168.
[21]. M. Karelson, V. S. Lobanov, A. R. Katritzky, *Chem. Rev.*, **1996**, *96*, 1027.
[22]. www.CACheSoftware.com
[23]. J. J. P. Stewart, *J. Comput. Chem.* **1989**, *10*, 209.
[24]. J. J. P. Stewart, *J. Compu. Aid. Mol. Design* **1990**, *4*, 1-105.
[25]. R. L. Mason, R. F. Gunst, J.T. Webster, *Commun. Statistics.* **1975**, *4*, 277.
[26]. D. C. Montgomery, E. A. Peck, Introduction to Linear regression analysis 2nd edition. *John Wiley*. New York. **1992**.
[27]. R. H. Myers, Classical and modern regression application. 2nd edition. *Duxbury press*. CA. **1990**.